

**Temporal variation and frequency dependence of seismic ambient noise on Mars
from polarization analysis**

Yudai Suemoto¹, Tatsunori Ikeda^{1,2}, Takeshi Tsuji^{1,2,3} *

¹ Department of Earth Resources Engineering, Kyushu University, Fukuoka 819-0395, Japan

² International Institute for Carbon-Neutral Energy Research (WPI-I2CNER), Kyushu University,
Fukuoka 819-0395, Japan

³ Disaster Prevention Research Institute, Kyoto University, Kyoto 611-0011, Japan

Corresponding author: Takeshi Tsuji (tsuji@mine.kyushu-u.ac.jp)

Contents of this file

Text S1 to S2

Table S1

Figure S1 to S3

Introduction

Text S1: Rotation of SEIS-VBB data to three orthogonal components

Text S2: Calculation of theoretical Rayleigh waves for a model of the InSight landing site

Table S1: Azimuth and dip angle of U, V, W component of seismometer

Figure S1: Power spectral density of seismic noise on Mars and Earth

Figure S2: Comparison of Rayleigh waves for fundamental, 1st higher and 2nd higher
modes for the baseline model of Knapmeyer-Endrun et al. (2017)

Figure S3: Temporal variations in the dominant back-azimuths and directional intensity
calculated from each 1-min segment

Text S1: Rotation of SEIS-VBB data to three orthogonal components

Table S1 shows the azimuth and dip angle of three components (U, V and W) of the triaxial seismometer of SEIS-VBB obtained from FDSN webservices of the Incorporated Research Institutions for Seismology (IRIS) (<http://ds.iris.edu/mda/XB/ELYSE/>). The original three components were rotated to construct seismic records with vertical and horizontal components. The relationship between original oblique components and vertical and horizontal components are given by;

$$\begin{pmatrix} D_E \\ D_N \\ D_Z \end{pmatrix} = \begin{pmatrix} -\sin(-\varphi_U)\cos(\theta_U) & \cos(-\varphi_U)\cos(-\theta_U) & \sin(-\theta_U) \\ -\sin(-\varphi_V)\cos(\theta_V) & \cos(-\varphi_V)\cos(-\theta_V) & \sin(-\theta_V) \\ -\sin(-\varphi_W)\cos(\theta_W) & \cos(-\varphi_W)\cos(-\theta_W) & \sin(-\theta_W) \end{pmatrix}^{-1} \begin{pmatrix} D_U \\ D_V \\ D_W \end{pmatrix}, \quad (1)$$

where D_U , D_V and D_W are original oblique components, φ and θ are azimuth and dip angles of three axes of seismometer, respectively, and D_E , D_N and D_Z are two horizontal (east-west and north-south) and one vertical components after rotation.

Table S1. Azimuth and dip angle of U, V, W component of seismometer

	Azimuth [°]	Dip [°]
U	135.1	-29.4
V	15	-29.2
W	255	-29.7

Text S2: Calculation of theoretical Rayleigh waves for a model of the InSight landing site

To evaluate if the motion of Rayleigh waves is prograde or retrograde at each frequency, we calculated analytical solutions of Rayleigh waves for a model of the InSight landing site. We used the baseline layered velocity model of Knapmeyer-Endrun et al. (2017), which includes an intermediate regolith thickness of 10 m. For the model, we computed analytical solutions of Rayleigh waves: phase velocity dispersion curve (Figure S2a), relative amplitude for vertical and horizontal components (Figures S2b and S2c), and ellipticity (Figure S2d) by DISPER80 (Saito 1988). The calculated ellipticities for each mode indicate that fundamental and 2nd higher modes of Rayleigh waves have retrograde motions (negative value of ellipticity), while 1st higher mode of Rayleigh waves has prograde motions (positive value of ellipticity) at most frequencies (Figure S2d). The relative amplitude of each mode for a vertical component, which can be calculated by the amplitude response (A_R) (Harkrider, 1970; Tokimatsu, 1997) divided by the square root of wavenumber (k), indicates fundamental mode of Rayleigh waves is mostly dominant in our analyzed frequency range. In the frequency ranges from 4.8 to 5.6 Hz and 7.4 to 8.0 Hz, 1st higher mode is dominant but 1st higher mode has retrograde motions in the frequency range from 7.4 to 7.9 Hz. On the other hand, relative amplitude of horizontal component indicates fundamental mode is dominant in horizontal component Rayleigh waves. These results suggest that Rayleigh waves would have mostly retrograde motions in the analyzed frequency range but in higher than 4 Hz, Rayleigh waves could have prograde motions as 1st higher mode is dominant in vertical component of Rayleigh waves.

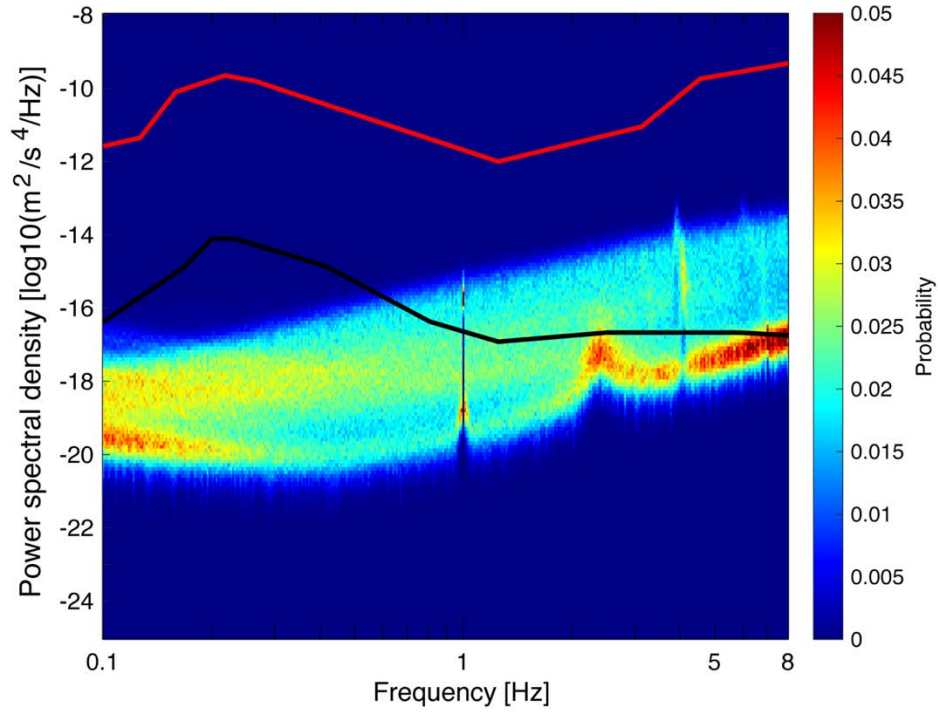


Figure S1. Power spectral density of seismic noise on Mars and Earth. Color counter shows the probability density function of Martian vertical seismic noise by InSight. We computed power spectral densities from each 10-min segment between Sols 75 and 211. Red and white lines show the Earth high noise model and the low noise model, respectively (Peterson, 1993).

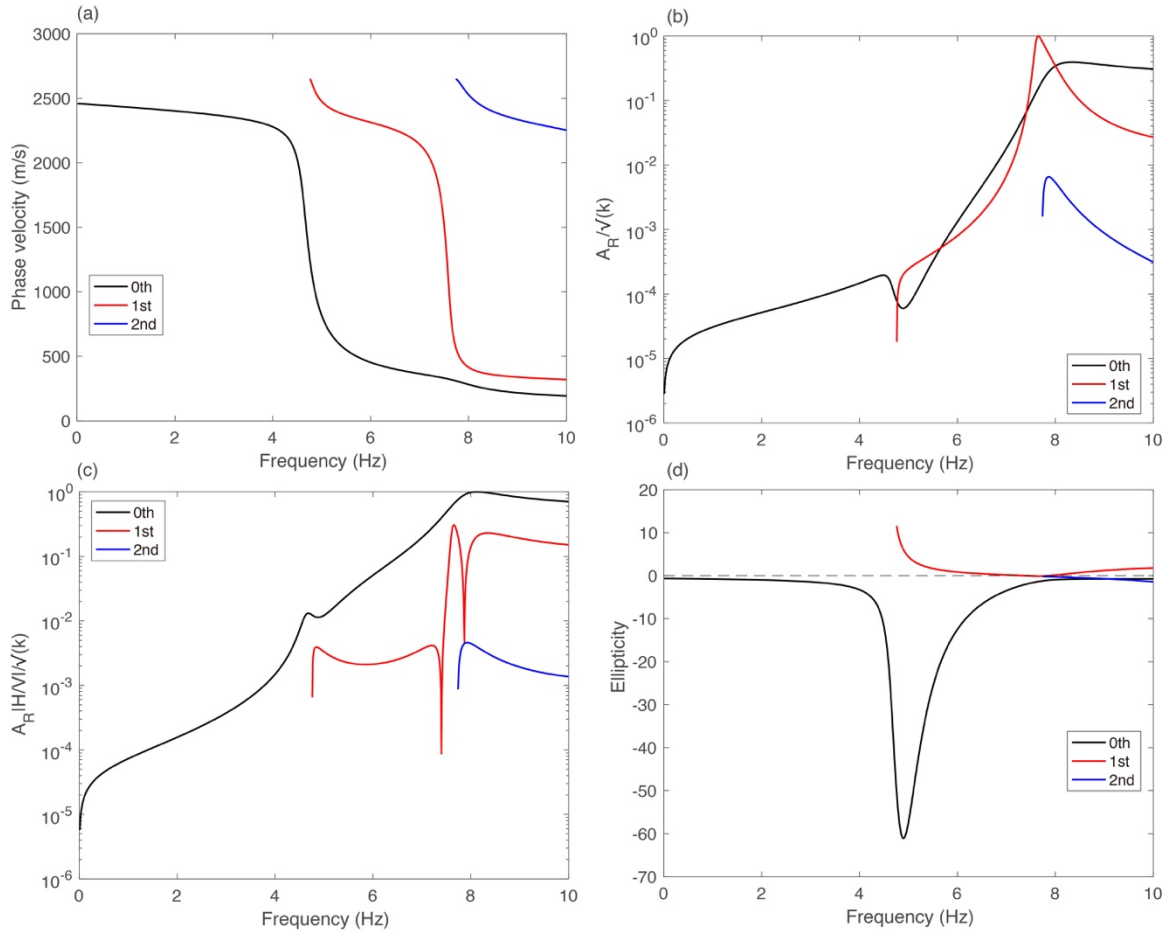


Figure S2. Comparison of Rayleigh waves for fundamental, 1st higher and 2nd higher modes for the baseline model of Knapmeyer-Endrun et al. (2017). (a) Phase velocity dispersion curve, (b) relative amplitude for vertical component, (c) relative amplitude for horizontal component calculated by multiplying absolute value of ellipticity (H/V) with the vertical response, and (d) ellipticity. Values in panels (b) and (c) are normalized by the maximum values. Negative values of ellipticity represent retrograde motions, while positive values indicate prograde motions.

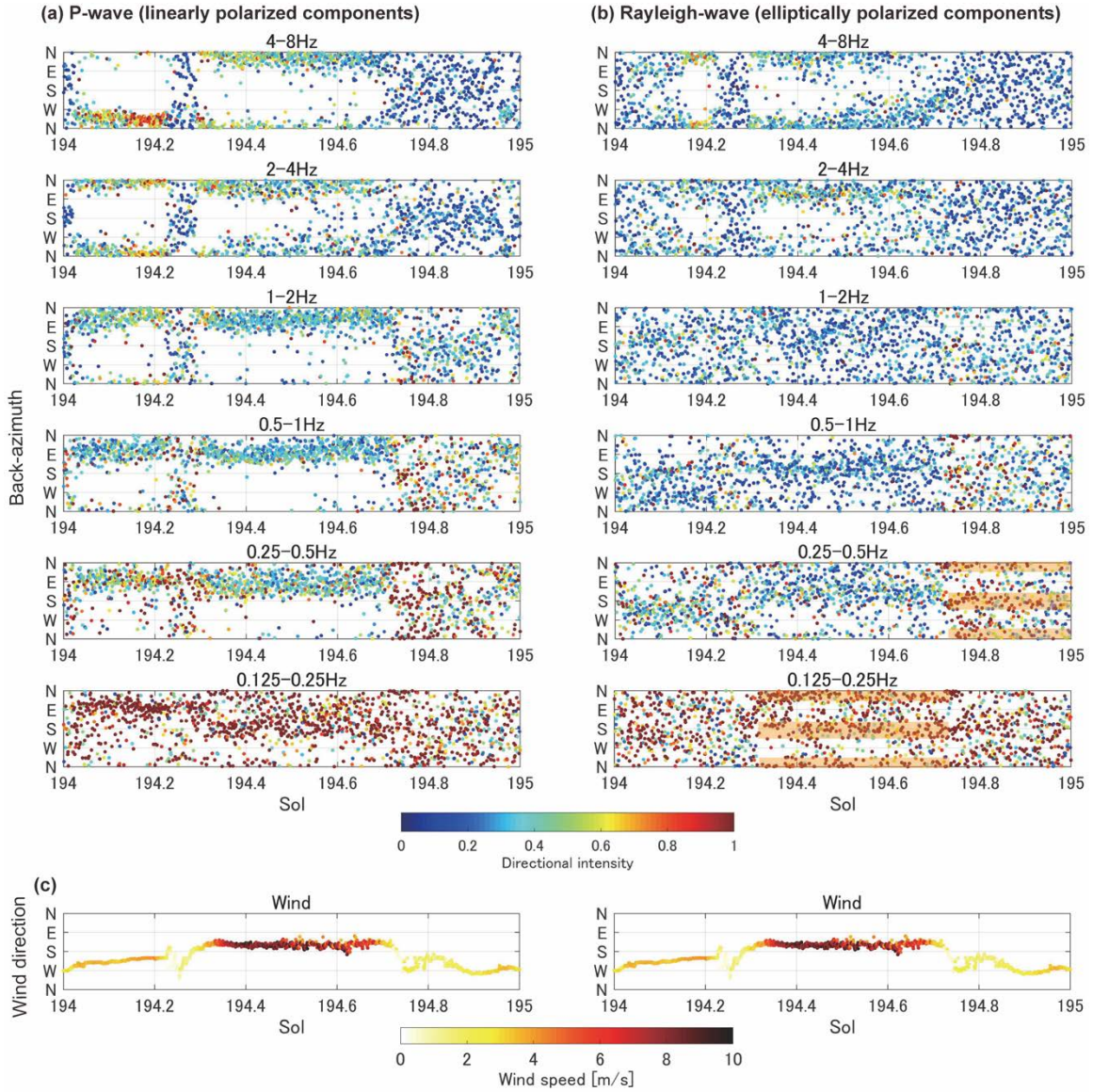


Figure S3. Temporal variations in Sol 194 in the dominant back-azimuths and directional intensity of (a) P-waves (linearly polarized components) and (b) Rayleigh waves (elliptically polarized components) calculated from each 1-min segment. Red shaded areas in panel (b) indicate dominant back-azimuths of low-frequency Rayleigh wave showing 180 degree ambiguity. (c) The wind speed and direction during the same period.